# IRAQI JOURNAL OF APPLIED PHYSICS LETTERS

The Iraqi Journal of Applied Physics Letters (IJAPLett) is a peer reviewed journal of high quality devoted to the publication of original research letters from applied physics and their broad range of applications. IJAPLett publishes quality original research letters in physics and its applications in the broadest sense. It is intended that the journal may act as an interdisciplinary forum for physics and its applications. Innovative applications and material that brings together diverse areas of physics are particularly welcome. IJAPLett aims to disseminate knowledge; provide a learned reference in the field; and establish channels of communication between academic and research experts, policy makers and executives in industry, commerce and investment institutions. IJAPLett is a quarterly specialized periodical dedicated to publishing original letters in: Alternative & Renewable Energy, Applied Mechanics & Thermodynamics, Applied Optics & Optical Design, Biophysics & Bioengineering, Cryptography & Applications, Electromagnetic Fields, Electronic Materials & Devices, Energy Generation & Conversion, Fluids Physics & Mechanics, Imaging, Microscopy & Spectroscopy, Laser Physics & Applications, Magnetism & Applications, Instrumentation, Measurements & Metrology, Nanostructures & Applications, Nonlinear & Ultrafast Optics, Nuclear Physics & Engineering, Optical Communications & Systems, Optoelectronics Devices & Applications, Organic Materials, Devices & Applications, Physical Chemistry & Biochemistry, Plasma, Discharge Physics & Applications, Quantum Physics & Spectroscopy, RF & Digital Communications, Semiconductors & Devices, Simulation & Modeling Research, Solar Energy & Devices, Solid State Physics & Applications, Structure & Properties of Matter, Superconductivity & Related Devices, Surfaces, Interfaces & Films, Thin Films & Applications, and Vacuum Science & Technology.

ISSN (Print)
**1999-656X**
ISSN (Online)
**2958-6488**

## EDITORIAL BOARD


| | | | | |
|---|---|---|---|---|
| **Oday A. HAMMADI** | Asst. Professor | Editor-in-Chief | Molecular Physics | IRAQ |
| **Walid K. HAMOUDI** | Professor | Member | Laser Physics | IRAQ |
| **Dayah N. RAOUF** | Asst. Professor | Member | Laser and Optics | IRAQ |
| **Raad A. KHAMIS** | Asst. Professor | Member | Plasma Physics | IRAQ |
| **Raid A. ISMAIL** | Professor | Member | Semiconductor Physics | IRAQ |
| **Kais A. AL-NAIMEE** | Professor | Member | Quantum Physics | IRAQ |
| **Haitham M. MIKHLIF** | Lecturer | Managing Editor | Molecular Physics | IRAQ |
| **Waleed N. RAJA** | Assistant Professor | Member | Radiation Physics | IRAQ |
| **Mahdi S. EDAN** | Assistant Professor | Member | Applied Physics | IRAQ |
| **Ali J. MOHAMMED** | Assistant Professor | Member | Thin Film Technology | IRAQ |
| **Falah H. ALI** | Assistant Professor | Member | Molecular Physics | IRAQ |


**Editorial Office**:
P. O. Box 88052, Baghdad 12631, IRAQ
Website: www.iraqiphysicsjournal.com
Emails: editor@iraqiphysicsjournal.com, editor_ijap@yahoo.co.uk, ijaplett.editor@gmail.com

## ADVISORY BOARD


| | |
|---|---|
| **Andrei KASIMOV**, Professor, Institute of Material Science, National Academy of Science, Kiev, | UKRAINE |
| **Ashok KUMAR**, Professor, Harcourt Butler Technological Institute, Kanpur, Uttar Pradesh 208 002, | INDIA |
| **Chang Hee NAM**, Professor, Korean Advanced Institute of Science and Technology, Daehak-ro, Daejeon, | KOREA |
| **Claudia GAULTIERRE**, Professor, Faculty of Sciences and Techniques, University of Rouen, Rouen, | FRANCE |
| **El-Sayed M. FARAG**, Professor, Department of Sciences, College of Engineering, AlMinofiya University, | EGYPT |
| **Gang XU,** Assistant Professor, Department of Engineering and Physics, University of Central Oklahoma, | U.S.A |
| **Heidi ABRAHAMSE**, Professor, Faculty of Health Sciences, University of Johannesburg, | S. AFRICA |
| **Madis-Lipp KROKALMA**, Professor, School of Science, Tallinn University of Technology, 19086 Tallinn, | ESTONIA |
| **Mansoor SHEIK-BAHAE**, Associate Professor, Department of Physics, University of New Mexico, | U.S.A |
| **Mohammad Robi HOSSAN,** Assistant Professor, Dept. of Eng. and Physics, Univ. of Central Oklahoma, | U.S.A |
| **Morshed KHANDAKER,** Associate Professor, Dept. of Engineering and Physics, Univ. of Central Oklahoma, | U.S.A |
| **Qian Wei Chang**, Professor, Faculty of Science and Engineering, University of Alberta, Edmonton, Alberta, | CANADA |
| **Sebastian ARAUJO**, Professor, School of Applied Sciences, National University of Lujan, Buenos Aires, | ARGENTINA |
| **Shivaji H. PAWAR**, Professor, D.Y. Patil University, Kasaba Bawada, Kolhapur-416 006, Maharashtra, | INDIA |
| **Xueming LIU**, Professor, Department of Electronic Eng., Tsinghua University, Shuang Qing Lu, Beijing, | CHINA |
| **Yanko SAROV**, Assistant Professor, Micro- and Nanoelectronic Systems, Technical University Ilmenau, | GERMANY |
| **Yushihiro TAGUCHI**, Professor, Dept. of Physics, Chuo University, Higashinakano Hachioji-shi, Tokyo, | JAPAN |

SPONSORED AND PUBLISHED BY
**AMERICAN QUALITY FOR SCIENTIFIC PUBLISHING INC.**
1479 South De Gaulle Ct, Aurora, CO 80018, United States

# IRAQI JOURNAL OF APPLIED PHYSICS LETTERS

ISSN (Print): 1999-656X, ISSN (Online): 2958-6488

## INSTRUCTIONS TO AUTHORS

**CONTRIBUTIONS**

Contributions to be published in this journal should be original research works, i.e., those not already published or submitted for publication elsewhere, individual papers or letters to editor.
Manuscripts should be submitted to the editor at the mailing address:

**Iraqi Journal of Applied Physics Letters, Editorial Board, P. O. Box 88052, Baghdad 12631, IRAQ**
**Website: www.iraqiphysicsjournal.com**
**Email: editor@iraqiphysicsjournal.com, editor_ijap@yahoo.co.uk, ijaplett.editor@gmail.com**

**MANUSCRIPTS**

Two hard copies with soft Word copy on a CD or DVD should be submitted to Editor in the following configuration:

- **One-column** Double-spaced one-side A4 size with 2.5 cm margins of all sides
- Times New Roman font (16pt bold for title, 14pt bold for names, 12pt bold for headings, 12pt regular for text)
- Manuscripts presented in English only are accepted.
- English abstract not exceed 100 words
- 4 keywords (at least) should be maintained on (PACS preferred)
- Author(s) should express all quantities in SI units
- Equations should be written in equation form (*italic* and symbolic) NOT in plain text
- Tables and Figures should be separated from text and placed in new pages after the references
- Charts should be indicated by the software used for generating them (e.g., Excel, MATLAB, Grapher, etc.)
- Figures and diagrams can be submitted in original colored forms for assessment and they will be returned to authors after provide printable copies
- Only original or high-resolution scanner photos are accepted
- For electronic submission, articles should be formatted with MS-Word software.

**AUTHOR NAMES AND AFFILIATIONS**

It is IJAPLett policy that all those who have participated significantly in the technical aspects of a paper be recognized as co-authors or cited in the acknowledgments. In the case of a paper with more than one author, correspondence concerning the paper will be sent to the first author unless staff is advised otherwise.
Author name should consist of first name, middle initial, last name. The author affiliation should consist of the following, as applicable, in the order noted:
- Company or college (with department name or company division), Postal address, City, Governorate or State, zip code, Country name, contacting telephone number, and e-mail

**REFERENCES**

The references should be brought at the end of the article, and numbered in the order of their appearance in the paper. The reference list should be cited in accordance with the following examples:
[1] X. Ning, R. Benford and M.R. Lovell, "On the Sliding Friction Characteristics of Unidirectional Continuous FRP Composites", *J. Tribol. Func. Mater.*, 124(1) (2002) 5-13.
[2] M. Barnes, "Stresses in Solenoids", *J. Appl. Phys.*, 48(5) (2001) 2000–2008.
[3] J. Jones, **"Contact Mechanics"**, Cambridge University Press (Cambridge, UK) (2000), Ch.6, p.56.
[4] Y. Lee, S.A. Korpela and R. Horne, "Structure of Multi-Cellular Natural Convection in a Tall Vertical Annulus", Proceedings of 7$^{th}$ International Heat Transfer Conference, U. Grigul et al., eds., Hemisphere (Washington DC), 2 (1982) 221–226.
[5] M. Hashish, "Waterjet Technology Development", High Pressure Technology, PVP-Vol. 406 (2000) 135-140.
[6] D.W. Watson, "Thermodynamic Analysis", ASME Paper No. 97-GT-288 (1997).
[7] C.Y. Tung, "Evaporative Heat Transfer in the Contact Line of a Mixture", Ph.D. thesis, Rensselaer Polytechnic Institute, Troy, NY (1982).

**PROOFS**

Authors will receive proofs of papers and are requested to return one corrected copy as a WORD file on a compact disc (CD) or by email. New materials inserted in the original text without Editor's permission may cause rejection of paper unless the handling editor is informed.

**COPYRIGHT FORM**

Author(s) will be asked to sign the IJAPLett Copyright Form and hence transfer copyrights of the article to the Journal soon after acceptance of it. This will ensure the widest possible dissemination of information.

**OFFPRINTS**

Authors will receive electronic offprint free of charge and any additional reprints can be ordered.

**SUBSCRIPTION AND ORDERS**

Annual fees (4 issues per year) of subscription are:
**50** US$ for individuals inside Iraq; **200** US$ for institutions inside Iraq;
**100** US$ for individuals abroad; **300** US$ for institutions abroad.

# Analysis of Paschen's Curve of Plasma Sputtering System Employing Closed-Field Unbalanced Dual Magnetron Assembly

**Hasan M. Jasim, Raad H. Abd**

Department of Physics, College of Education, Mustansiriyah University, Baghdad, IRAQ

**Abstract**

The effects of closed-field unbalanced dual magnetrons on the performance of plasma sputtering system were studied. These effects were introduced by comparing the obtained Paschen's curve in existence and absence of magnetrons. The distribution of magnetic fields between the magnetrons was introduced to optimize the closed-field unbalanced configuration. Characterization of Paschen's curve as well as discharge current with gas pressure at different distances between the discharge electrodes was introduced. Also, the current-voltage characteristics were introduced at the optimum operation conditions.

**Keywords:** Physical vapor deposition, Sputtering, Magnetron sputtering, Paschen's law

**Received**: 03 March 2023; **Revised:** 28 April 2023; **Accepted:** 03 May 2023; **Published:** 1 June 2023

## 1. Introduction

In sputtering, at low kinetic energies (energies between 0 and about 50 eV), the ion does not have sufficient energy to dislodge the target atoms and thus the ejection of target particles occurs only for very special collision geometries [1-4]. With moderate energies (between 50 and roughly 1 keV), the ions impact dislodge "knock-on" atoms into the target, which by their turn will dislodge other target atoms [5]. Several studies showed that the ion energies must exceed four times the binding energy of the atoms of the target surface to induce sputtering. This induces collision cascade that eject atoms, ions, electrons and neutrals from the first 10 to 50Å of the surface of a target [6-9].

The breakdown voltage ($V_B$) depends on the product of pressure ($p$) and electrode separation ($d$) as this product is denoted as "*pd*", while this voltage weakly depends on the cathode material that defines the emission coefficient of secondary electrons [10-13]. As well, the breakdown voltage is proportional to the product *pd* at large values of this product and the electric field ($E=V/d$) is scaled linearly with the pressure [14]. In case of small values of the product *pd*, only few collisions occur and higher voltage is applied to increase the probability of breakdown per collision. Hence, the minimum voltage required to ignite the discharge of a gas sample of pressure $p$ over a distance $d$ is defined at the minimum of Paschen's curve, where

$$pd|_{V_{min}} = \frac{1}{A} log\left(1 + \frac{1}{\gamma_e}\right) \quad (1)$$

If the pressure and/or separation distance is too large, ions generated in the gas are slowed by inelastic collisions so that they strike the cathode with insufficient energy to produce secondary electrons. In most sputtering glow discharges, the discharge starting voltage is relatively high.

Eventually, an avalanche occurs in which the ions striking the cathode release secondary electrons, which form more ions by collision with neutral gas atoms. These ions then return to the cathode, produce more electrons. When the number of electrons generated is just sufficient to produce enough electrons to regenerate the same number of electrons, the discharge is self-sustaining. The gas begins to glow, the voltage drops, and the current rises abruptly [15]. This is called the "normal glow". The color of this luminous region is characteristic of the excitation gas used. Since the secondary electron emission ratio of most

 © All Copyrights are reserved 

materials is of the order of 0.1, more than one ion must strike a given area of the cathode to produce another secondary electron. The bombardment of the cathode in the normal glow region self-adjusts in the area to accomplish this. Initially, the bombardment is not uniform, but concentrated near the edges of the cathode or at other irregularities on the surface. As more power is supplied, the bombardment increasingly covers the cathode surface until a nearly-uniform current density is achieved [14].

## 2. Experimental Part

The electrodes were connected to a DC power supply to provide the electrical power required for discharge. The lower electrode (anode) could be move vertically with respect to the fixed upper electrode (cathode) to adjust the separation of the two electrodes from 1 to 8 cm.

Pure argon gas was used to produce the discharge plasma for sputtering. A DC power supply providing voltage up to 6kV was used for electrical discharge between the electrodes and both breakdown voltage (up to 1 kV) and discharge current (up to 100 mA) were monitored by two digital voltmeter and ammeter, respectively.

First, the magnetic field intensity of each magnetron was measured individually, and second, the magnetic field intensity between both magnetrons was measured too. In the second case, the magnetrons were maintained parallel to each other and the probe was positioned between them using an adjustable clamp. Measurements were carried out over all the distance between the two magnetrons in all coordinates in order to determine the

## 3. Results and Discussion

In order to determine the optimum distance between two magnetrons, the magnetic field intensity was measured at the midpoint along the distance between the two magnetrons and at 2.2 cm from the edge of the electrode and the results are shown in Fig. (1). The maximum was observed at 4 cm, which can be considered as the optimum distance, while the minimum was measured at ≥ 8 cm. The diameter of the measuring probe is 0.8 cm, therefore, the minimum distance was 2 cm in order to locate the measuring probe at the midpoint. The behavior shown in the figure below is attributed to the interference between the lines of the magnetic field, i.e., the maximum interference occurs at the midpoint of 4cm separation, whereas this interference decreases as the two magnetrons move away from each other reaching to “no interference” condition at ≥ 8 cm separation.

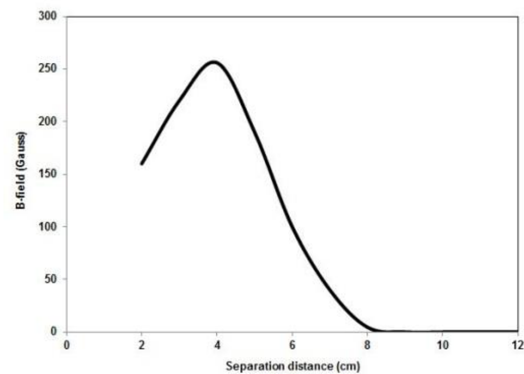


**Fig. (1) Variation of magnetic field intensity along the vertical distance separating the two magnetrons**

The electrons are unable to travel perpendicular to the magnetic field lines over distances greater than Larmor radius, therefore, they are confined. The electric field on the other hand causes the electrons to move in the direction perpendicular to both the electric field and the magnetic field (E×B or Hall drift) [16]. The combination of the electron confinement and the E×B drift ensures that the electrons have a much longer mean free path in the plasma than in conventional glow discharges, giving rise to more ionization collisions, and consequently higher ion fluxes [17]. These ion fluxes are highest in between the magnets, hence most of the target material is sputtered there. This gives a characteristic feature of conventional planar magnetrons called the racetrack [18]. This racetrack generally limits the complete target utilization, resulting in higher working costs [19]. This problem can be overcome by using rotatable magnetrons. Instead of a cylindrical inner magnet and an outer magnet ring, these magnetrons consist of a central bar shaped magnet surrounded by a rectangular

shaped magnet configuration around which a cylindrical target rotates. This greatly enhances the utilization of the target and is therefore much more interesting for industrial applications [20].

The sputtering electrons are assumed to be trapped near the cathode by the magnetic field of the magnetron in order to increase the path length of these electrons. Therefore, the maximum interference between the two fields is not preferred for such purpose because the electrons would not be seized near the cathode. Instead, these electrons may be drifted by the interfered lines away from the cathode.

Sputtering of a target atom is just one of the possible effects resulting from the surface ion bombardment. Aside from sputtering, the second important process is the emission of secondary electrons from the target surface, which play a fundamental role in keeping the sputtering process itself. Figure (2) shows Paschen's curve for both cases of using and not using the magnetron at the upper electrode (cathode). As clearly shown, the effect of using magnetron lies in decreasing the breakdown voltage to about 15% of its initial (maximum) value, while the minimum voltage was decreased to seventh its value in absence of magnetron. However, Paschen's curves of both cases are identical with different minima, as the value of "*p.d*" product was 1.1 mbar.cm when no magnetron is used and 1.4 mbar.cm when a magnetron is used.

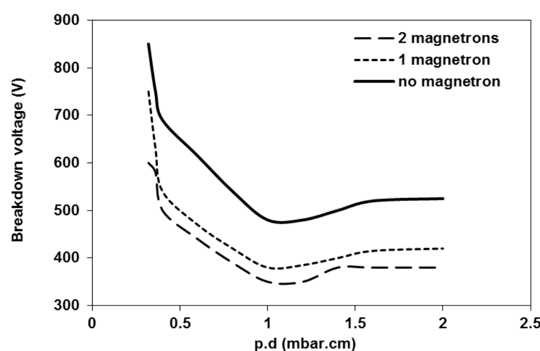


**Fig. (2) Paschen's curve for the constructed plasma sputtering system with and without magnetron**

A disadvantage of the magnetron sputtering configuration is that the plasma is confined near the cathode and is not available to active reactive gases in the plasma near the substrate for reactive sputter deposition. This difficulty can be overcome using an unbalanced magnetron configuration, where the magnetic field is such that some electrons can escape from the cathode region [21]. An unbalanced magnetron (UBM) has a proper magnetic field configuration in which a finite degree of the field lines from the outer magnetic pole diverge to the substrate, though the rest of the lines finish on the inner pole behind the target. Sufficient plasma density and a positive ion current on a metallic substrate even at a large distance from the target can be achieved in the unbalanced magnetron as compared with the balanced one [22,23].

The plasma sputtering system was then characterized by the relation of discharge current to the gas pressure inside the chamber at different inter-electrode distances, as shown in Fig. (3). Again, all curves are identical with the discharge current shifted upward on the vertical axis. As the distance between the electrodes is decreased, the current density from electron current emitted from the cathode $j_e(0)$ is increased because less number of electrons are able to reach the anode and hence lower current flows. However, compensation is required between gas pressure and distance to work at a given discharge current before converting into decreasing current as saturation is reached.

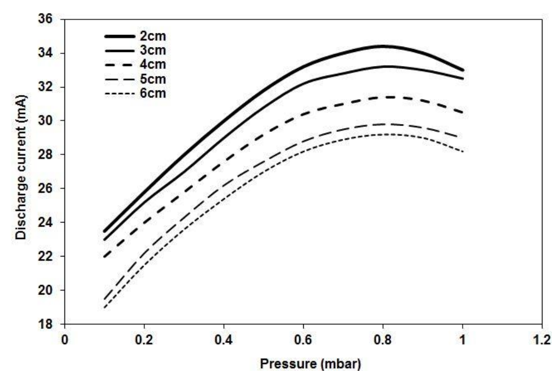


**Fig. (3) Variation of discharge current with increasing gas pressure for different inter-electrode distances (*d*)**

The plasma pressure will also have an impact on the sputtering process. Higher pressure means high density of gas molecules

in the chamber. As a consequence, this will lead to higher electron density and ion density in the plasma. The high electron and ion density will increase the bombardment counts and also the probability of collision between particles. The applied voltage will have an impact on the charged particles density and the energetic level of the charged particles. The density of ions is mainly related with the power input to the plasma. Usually, one thirtieth of the discharge energy will be transformed into ionization process. However, the applied voltage shouldn't reach too high for avoiding the implantation of ions.

## 4. Conclusion

Referring to the results obtained from this work, the home-made dc magnetron plasma sputtering system was characterized to introduce its performance in accordance to magnetic field distribution, electrical characteristics, Paschen's law and governing properties of such deposition systems. Results have showed that using magnetron at the cathode of discharge configuration highly has affected these operation characteristics as the breakdown voltage was decreased, the minimum point was little shifted upward, . This system was found to satisfy the requirements for deposition of high-quality thin films from different materials.

## References


[1] E.D. McClanahan and N. Laegreid, Topics in Appl. Phys., 64 (1991) 339-377.
[2] D. Rademacher, T. Zickenrott, M. Vergöhl, Thin Solid Films 532 (2013) 98–105.
[3] J.-S. Baek and Y.J. Kim, Cooling Effect Enhancement In Magnetron Sputtering System, 5th Inter. Conf. on CFD in the Process Industries CSIRO, Melbourne, Australia 13-15 December 2006, 1-5.
[4] P.J. Kelly and R.D. Arnell, Vacuum 56 (2000) 159-172.
[5] R.D. Arnell and P.J. Kelly, Surf. Coat. Technol., 112 (1999) 170–176.
[6] J. Walkowicz et al., Tribologia, 6 (2006) 163-174.
[7] D.E. Ashenford et al., Surf. Coat. Technol., 116-119 (1999) 699-704.
[8] P. Sigmund, **Topics in Applied Physics: Sputtering by Particle Bombardment I**, ed. R. Behrisch, Vol. 47, Springer-Verlag (Berlin) 1981.
[9] F. Taherkhani and A. Taherkhani, Transaction B: Mechanical Engineering, 17(4) (2010) 253-263.
[10] G.K. Wehner and G.S. Anderson, **Vacuum Technology, Thin Films and Sputtering: An Introduction**, ed. R. V. Stuart, Academic Press, New York, 1983.
[11] A. Bogaerts et al., Spectrochimica Acta Part B 57 (2002) 609–658.
[12] E.F. Kotp and A.A. Al-Ojeery, Australian J. Basic Appl. Sci., 6(3) (2012) 817-825.
[13] S.D. Personick, Bell System Tech. J., 50(10) (1971) 3075-3095.
[14] J.-C. Wang et al., J. Appl. Phys., 113 (2013) 033301
[15] L.M. Isola, B.J. Gomez and V. Guerra, J. Phys. D: Appl. Phys., 43 (2010) 015202.
[16] T.E. Sheridan, M.J. Goeckner, and J. Goree, J. Vac. Sci. Technol. A 16(4) (1998) 2173-2176.
[17] F. Papa et al., Thin Solid Films, 520(5) (2011) 1559-1563.
[18] B. Liebig et al., Surf. Coat. Technol., 205 (2011) S312–S316.
[19] P.J. Kelly and R.D. Arnell, Surf. Coatings Technol., 112 (1999) 170-176.
[20] A.S. Penfold, in **Handbook of Thin Film Process Technology**, IOP (1995), sec. A.3.2, p. 1.
[21] B. Window and N. Savvides, J. Vac. Sci. Technol., A 4(2) (1986) 196.
[22] T. Makabe and Z. Petrovic, **Plasma Electronics: Applications in Microelectronic Device Fabrication**, Taylor & Francis, New York (2006) 301.
[23] B.T. Chiad, M.K. Khalaf, F.J. Kadhim, O.A. Hammadi, Characteristics and Operation Conditions of a Closed-Field Unbalanced DC Magnetron Plasma Sputtering System, J. Ind. Eng. Sci., accepted for publication, to appear in 2015.


 © All Copyrights are reserved 

# Closed-Field Unbalanced Dual Magnetron Assembly for Plasma Sputtering Systems

**Ali M. Ghafoori[1], Omar S. Habeeb[2], Mohammed A. Hussain[1]**

[1] Department of Electrical Engineering, College of Engineering, University of Anbar, Ramadi, IRAQ
[2] Department of Software Engineering, College of Engineering, University of Baghdad, Baghdad, IRAQ

**Abstract**
In this work, a closed-field unbalanced dual magnetron assembly was designed, constructed and characterized. This assembly can be successfully used in plasma sputtering system to improve the electrical characteristics of the plasma. This improvement was shown by the Langmuir probe diagnostics of the plasma and the values of plasma parameters, such as electron and ion temperatures and densities. The applicability of such design may enhance the whole sputtering process and the production of nanoscale structures with low cost, high purity and good properties.

**Keywords:** Magnetron sputtering; Plasma parameters; Langmuir diagnostics; Glow discharge
**Received**: 02 February 2023; **Revised:** 08 May 2023; **Accepted:** 15 May 2023; **Published:** 1 June 2023

## 1. Introduction

Different sputtering configurations were developed during the last five decades due to the technological advances in the power supplies, vacuum pumps and other components [1-4]. All these developments are aiming to increase the sputtering rate, the available deposition area, and the ionization as well as to decrease plasma heating of the substrate and working gas pressures, in addition to facilitate the coating of complex substrate shapes and deposit non-conductive or compound thin films [5-9].

The confinement of electron is based on the Lorentz force given by the vector cross product of both electric ($\vec{E}$) and magnetic ($\vec{B}$) fields [10]. Since $\vec{E}$ is perpendicular to the target surface, application of a $\vec{B}$ field tangential to the surface gives the electron a component of velocity parallel to the target [11,12]. Forcing the electrons in plasma to move in helical path results in a great increase in a probability that an electron will have a collision with a gas atom, leading to either exciting or ionizing the atom before being scattered out of the plasma region [13]. This effect can be used to form very dense, low-impedance plasma. A single electron from the target can generate at least 10 electron-ion pairs in the volume of magnetized plasma [14].

Magnetron sputtering (especially closed-field unbalanced magnetron configuration) has gained wide acceptance in both research and commercial purposes and is routinely used in different industries like cutting tools, forming tools, semiconductor, optical glass coating, decorative, biomedical, and tribology applications [15]. Depending on the configuration of the magnets, a magnetron can be either “balanced” or “unbalanced”. A balanced magnetron implies that all magnetic field lines are closed in on themselves, while an unbalanced magnetron has open field lines that are directed towards the chamber walls (“type 1”) or towards the substrate (“type 2”) [16].

In case of planar circular magnetron – which is used in the present work – two round magnets are placed behind the target, as can be seen in the figure below and formation of an erosion profile known as “racetrack” is induced by the non-uniform ion bombardment across the target surface [17]. For balanced magnetrons, both magnets have the same magnet strength that results in strongly confined plasma near the target region [18]. Consequently, only a few charged particles reach the substrate, which might be useful in

 © All Copyrights are reserved 

the case where low energetic bombardment is mandatory as in the case of polymeric substrates, but it is a drawback when energetic ion/electron bombardment in the anode surface is needed because the bombardment with energetic particles (ions or electrons) influence the growth of thin films [19-22].

In the closed-field configuration, the lines of magnetic field are linked between the magnetrons, therefore, losses of secondary electrons towards the walls of chamber are low and the substrate is immersed in the high-density plasma region [23]. The advantage of this configuration when compared to the mirrored one is realized by the ion-to-atom ratio incident at the substrate (2-3 times greater) at the same conditions [24]. This advantage is observed when comparing to single unbalanced magnetron configuration as well as when the distance from the target is increased [25].

Accordingly, the major advantages of closed-field unbalanced magnetrons are high uniformity of the deposited film thickness, high stability of deposition rate for >100 hours uninterrupted production, good reproducibility of layer properties for long periods of time, good adhesion and high density of deposited coatings, the ability to deposit all kinds of metals including high melting-point metals, metal alloys and compounds with precise control of coating composition, the ability to deposit metal oxides, nitrides, carbides, etc. with precise control of layer stoichiometry, and the ability to deposit tailored design coatings like multicomponent, multilayer, gradient, composite coating, etc. [26].

In this work, a closed-field unbalanced dual magnetron assembly was designed, constructed and characterized to be used in plasma sputtering system to improve the electrical characteristics of the plasma. This improvement was shown by the Langmuir probe diagnostics of the plasma and the values of plasma parameters, such as electron and ion temperatures and densities.

## 2. Experimental Part

Two closed-field unbalanced magnetrons were employed at the anode and cathode of plasma sputtering system. Electrodes (anode and cathode) were made of stainless steel and each was a disk of 8 cm in diameter and 4 mm in thickness. Two annular concentric magnets were placed behind each electrode to form the magnetron configuration. The outer diameters of the two magnets were 8 cm and 4 cm, while the inner diameters were 4 cm and 3.2, respectively. The electrodes were connected to a DC power supply to provide the electrical power required for discharge. The lower electrode (anode) could be move vertically with respect to the fixed upper electrode (cathode) to adjust the separation of the two electrodes from 1 to 8 cm.

Pure argon gas was used to produce the discharge plasma. A DC power supply up to 5 kV was used for electrical discharge between the electrodes and both breakdown voltage (up to 1 kV) and discharge current (up to 100 mA) were monitored by two digital voltmeter and ammeter, respectively. A current limiting resistor of 6.75 kW was connected in series to the discharge circuit in order to control the current flowing in the circuit. The discharge chamber was evacuated by a two-stage Leybold-Heraeus rotary pump and the vacuum inside chamber was measured by Pirani gauge connected to a vacuum controller from Balzers VWS 120. Argon gas was supplied to the chamber through a fine-controlled needle valve (0-160 ccm) to control the gas pressure inside the chamber.

## 3. Results and Discussion

According to the most common assumptions of probe theory, plasma is supposed to be homogenous and its dimensions are large when compared to the mean free path of the electrons, which is inversely proportional to the mean probability of electron collision. In low-pressure plasma (<0.2mbar), the mean free path of electrons must be sufficiently long but shorter than the distance between the electrodes.

Moving to the positive bias voltage region, the electron current is slowly increasing with

 © All Copyrights are reserved 

increasing bias voltage to reach a point at which, drastic increase in this current is observed. This behavior does not continue as it converts into slow increasing at a certain bias voltage known as “plasma potential” ($V_p$). At this point, the probe is immersed inside plasma and no sheath develops around the probe and the charges reach its surface because of their thermal motion. Thus, the probe collects the thermal flux of both electrons and ions. In consequence, the probe biased at the space plasma potential drains an electric current from the plasma even in the absence of potential difference between the conductor and the surrounding plasma. The measured values of floating and plasma potentials for the three working pressures are 5V and 40V, respectively.

Figure (1) explains the effect of variation in working pressure on the current-voltage characteristics of Langmuir probe diagnostics in unmagnetized glow-discharge plasma. As shown, increasing working gas pressure results in measuring higher probe current due to the increasing density of neutral gas atoms those subjected to collisions with the available charged particle and hence producing much more charged particles those composing the drained current. However, the behaviors of these characteristics are identical with upward shift at higher pressures, as mentioned above.

In order to introduce the effects of using magnetrons on the parameters of plasma, the Langmuir probe measurements were performed when only one magnetron used at the cathode and when dual magnetrons used and then compared the obtained results to those obtained when no magnetron used, as shown in Fig. (3).

It is clear that using only one magnetron at the cathode caused to decrease the drained current by the probe by about 12%. This decrease may be attributed to the role of this magnetron in trapping a fraction of the electrons in discharge volume near the cathode to increase the ionization rate of the neutral gas atoms and hence preventing the probe from collecting more electrons.

When dual magnetrons were used, the drained current by the probe was decreased by about 16% due to the roles of both magnetrons in trapping much more charged particles near the cathode and anode and hence reducing the number of particles passing the distance between the electrodes where the probe is placed. However, these roles could not prevent the discharge current from flowing between the electrodes but even these particles sustaining the discharge are accelerated by the both electric and magnetic fields to higher drift velocities that the probe could not attract them from their paths across the inter-electrode distance [27-29].

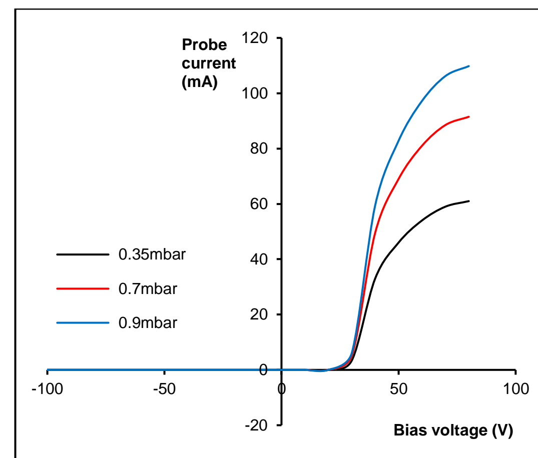


**Fig. (2) The effect of variation in working pressure on the current-voltage characteristics of Langmuir probe diagnostics in unmagnetized glow-discharge plasma**

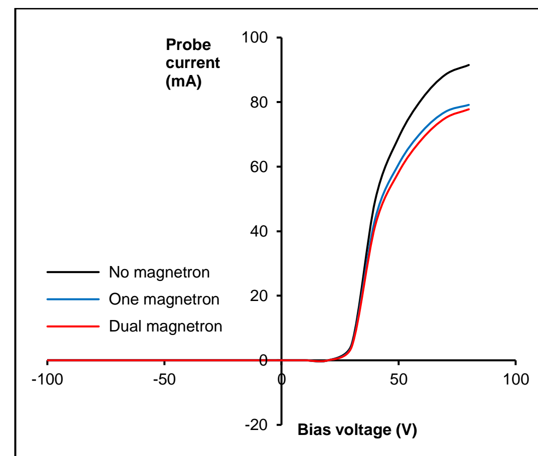


**Fig. (3) Current-voltage characteristics of Langmuir probe diagnostics in glow-discharge plasma at three different cases (no magnetron, using one magnetron at the cathode, and using dual magnetrons)**

## 4. Conclusion

From the results obtained in this work, the effect of the proposed configuration of closed-field unbalanced dual magnetrons on the electrical parameters of the discharge plasma

 © All Copyrights are reserved 

was introduced. This configuration of magnetrons caused to increase the ionization process by confining the charged particles (especially electrons) near the electrodes and hence the number of collisions of these particle with the neutral atoms provided to the vacuum chamber was increased too.

Using only one magnetron at the cathode caused to decrease the drained current by the probe by about 12%. This decrease may be attributed to the role of this magnetron in trapping a fraction of the electrons in discharge volume near the cathode to increase the ionization rate of the neutral gas atoms and hence preventing the probe from collecting more electrons. When dual magnetrons were used, the drained current by the probe was decreased by about 16% due to the roles of both magnetrons in trapping much more charged particles near the cathode and anode and hence reducing the number of particles passing the distance between the electrodes where the probe is placed.

## References

[1] M. Lieberman, A. Lichtenberg, **Principle of plasma discharge and Material**, New York, John-Wiley and Sons (1994).

[2] G. Seriamni et al., “plasma Charactersation of a DC closed field magnetron sputtering device”, ECA, 24B, 17 (2000).

[3] M. Ghoranneviss et al., “The effect of parameter of plasma of DC magnetron sputtering on properties of copper thin film deposited on glass”, XXVIIth ICPIG, Eindhoven, Netherlands (2005).

[4] C. Shon et al., IEEE Transactions on plasma science", 26(6) (1998).

[5] B. Chapman, **Glow Discharge Processes**, John-Wiley & Sons, NY (1980).

[6] R. Berry, P. Hall, and M. Harris, **Thin Film Technology**, van Nostrand Reinhold Company, New York (1968).

[7] K. Hinkel, **Magnetrons**, Cleaver-Hume Press Ltd., London, 1961.

[8] J. Vossen, **Thin Film Processes**, Academic Press, Inc., New York (1978).

[9] K. Wasa and S. Hayakawa, Rev. Sci. Instrum., 40(5) (1969) 693.

[10] B. Subramanian et al., Surf. Coat. Technol., 205(21-22) (2011) 5014–5020.

[11] A. Grill, **Cold Plasma in Materials Fabrication**, IEEE, New York, 1994.

[12] N. Kumari et al., Euro. Phys. J., 59(2) (2012), Article ID 20302, 7 pages.

[13] J.A. Thornton, J. Vac. Sci. Technol., 15(2) (1978) 171–177.

[14] S.Z. Wu, J. Appl. Phys., 98 (2005), Article ID 083301, 5 pages.

[15] T.E. Sheridan, M.J. Goeckner and J. Goree, J. Vac. Sci. Technol. A, 8(30) (1990) 8 pages.

[16] S.L. Rohde et al., Thin Solid Films, 193-194(1) (1990) 117–126.

[17] R.P. Howson, H.A. J’Afer and A.G. Spencer, Thin Solid Films, 193-194(1) (1990) 127–137.

[18] S.M. Borah et al., J. Phys. D: Appl. Phys., 41(19) (2008), Article ID 195205.

[19] X.B. Zhang, J.Q. Xiao, Z.L. Pei, et al., J. Vac. Sci. Technol. A 25, 209 (2007).

[20] I. Petrov, F. Abibi, J.E. Greene, et al., J. Vac. Sci. Technol. A 10, 3283 (1992).

[21] I. Ivanov, P. Kazansky, L. Hultman, et al., J. Vac. Sci. Technol. A 12, 314 (1994).

[22] S.M. Rossnagel and H.R. Kaufman, J. Vac. Sci. Technol. A 4, 1822 (1986).

[23] T.E. Sheridan and J. Goree, J. Vac. Sci. Technol. A 7, 1014 (1989).

[24] I. Petrov, I. Ivanov, V. Orlinov, and J. Kourtev, Contrib. Plasma Phys. 30, 223 (1990).

[25] P. Spatenka, J. Vlcek, and J. Blazek, Vacuum 55, 165 (1999).

[26] L. Gu and M.A. Lieberman, J. Vac. Sci. Technol. A 6, 2960 (1988).

[27] B.T. Chiad, M.K. Khalaf, F.J. Kadhim, O.A. Hammadi, Characteristics and Operation Conditions of a Closed-Field Unbalanced DC Magnetron Plasma Sputtering System, J. Ind. Eng. Sci., accepted for publication, to appear in 2015

[28] M.K. Khalaf, O.A. Hammadi, F.J. Kadhim, Representation of Magnetic Field Distribution of Dual Closed-Field Unbalanced Magnetrons Employed in Glow-Discharge Plasma Sputtering System, submitted to Photonic Spectra, 2014.

[29] F.J. Kadhim, M.K. Khalaf, O.A. Hammadi, Optical and Structural Properties of Nickel Oxide Thin Films Prepared by Closed-Field Unbalanced Dual-Magnetrons Sputtering Technique, J. Optoelectron. Photon., accepted for publication, to appear in 2015.

# Effect of Preparation Method on Crystalline Structure of Titanium Dioxide Nanoparticles

**Zahraa H. Zaidan[1], Oday A. Hammadi[2], Kasim H. Mahmood[1]**

[1] Department of Physics, College of Education for Pure Sciences, Tikrit University, Tikrit, IRAQ
[2] Department of Physics, College of Education, Al-Iraqia University, Baghdad, IRAQ

**Abstract**
In this work, titanium dioxide ($TiO_2$) nanoparticles were prepared by two different methods; solvothermal and dc reactive sputtering. The crystalline structures of these nanoparticles were determined by x-ray diffraction in order to introduce the effect of preparation method on the structural characteristics of these nanoparticles. In solvothermal method, the $TiO_2$ nanopowder was prepared as a nanopowder precipitated from an extract solution of banana peels and titanium isopropoxide. In dc reactive sputtering technique, the $TiO_2$ nanopowder was extracted from thin film samples deposited on glass substrates. Results showed that the crystalline structure of the nanopowder prepared by solvothermal method contains both anatase and rutile phases of $TiO_2$ with mixing ratio of 1:1, while the crystalline structure of the nanopowder prepared by dc reactive sputtering contains both anatase and rutile phases with mixing ratio of 2:1. As well, single phase (anatase) nanopowder was prepared by using heat sink method to prevent the thermal transition of anatase into rutile phase. Average crystallite size was determined for the three samples and found to be 38, 27 and 37 nm for 1:1, 2:1 and anatase samples, respectively. Accordingly, preparation method has an important role in determining the structural characteristics of the $TiO_2$ nanopowder and hence the preparation parameters should be sufficiently governed in order to control these characteristics.

**Keywords:** Titanium dioxide; Nanoparticles; Structural phase; Reactive sputtering; Solvothermal method
**Received**: 17 February 2023; **Revised:** 11 May 2023; **Accepted:** 18 May 2023; **Published:** 1 June 2023

## 1. Introduction

Crystallinity is an important factor to be considered in the optimization of the photodegradation efficiency [1,2]. It has been shown that amorphous $TiO_2$ has negligible photodegradation efficiency compared with $TiO_2$ of high crystallinity [3,4]. The low efficiency of amorphous $TiO_2$ is caused by the high recombination rate of electrons and holes due to the large amount of defects [5,6].

$TiO_2$ is close to be an ideal photocatalyst and the benchmark for photocatalysis performance [7,8]. $TiO_2$ is cheap, photostable in solution and nontoxic. Its holes are strongly oxidizing and redox selective [9]. For these reasons, several novel heterogeneous photocatalytic reactions have been reported at the interface of illuminated $TiO_2$ photocatalyst, and $TiO_2$-based photocatalysis has been researched exhaustively for environmental cleanup applications [10,11]. The single drawback is that it does not absorb visible light [12]. To overcome this problem, several methods including dye sensitization, doping, coupling and capping of $TiO_2$ are proposed [13].

In this work, titanium dioxide ($TiO_2$) nanoparticles were prepared by two different methods; solvothermal and dc reactive sputtering. The crystalline structures of these nanoparticles were determined by x-ray diffraction in order to introduce the effect of preparation method on the structural characteristics of these nanoparticles.

## 2. Experimental Part

Two methods were used in this work to prepare titanium dioxide ($TiO_2$) nanoparticles. In the first method, solvothermal method, the $TiO_2$ nanoparticles were synthesized from the titanium isopropoxide and banana peels. For more details on this work, see reference [14]. In the second method, dc reactive magnetron sputtering, a highly-pure titanium sheet was sputtered in presence of $Ar:O_2$ gas mixture inside a vacuum chamber at gas pressure of 0.5mbar and discharge current of 40mA to deposit $TiO_2$ thin films on glass substrates.

 © All Copyrights are reserved Printed in Iraq 

The deposited films were containing both rutile and anatase phases of $TiO_2$. In order to deposit $TiO_2$ films with only anatase phase, a heat sink was placed under the substrate to avoid the thermal transition of anatase into rutile phase. For more details on this technique, see references [9-13]. The nanopowder was extracted from the tin film samples by the conjunctional freezing-assisted ultrasonic extraction method [15].

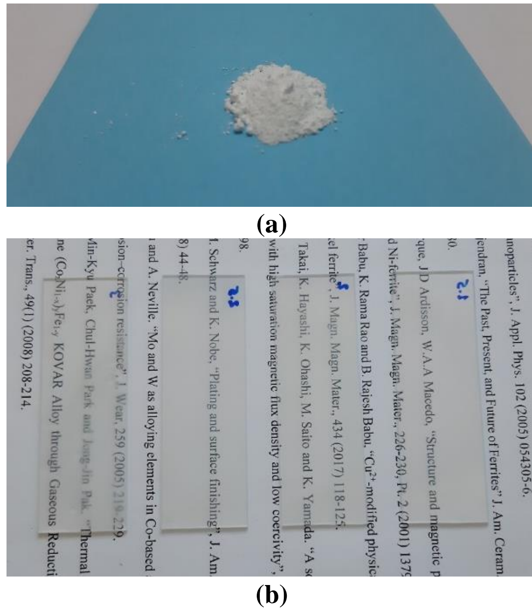

(a)

(b)

**Fig. (1) Photographs of nanopowder prepared by solvothermal method (a) and thin films prepared by dc reactive sputtering technique at different deposition times**

The crystalline structures of the prepared nanopowders were determined by the x-ray diffraction (XRD) patterns obtained using a Bruker D2 PHASER XRD system (Cu-Kα x-ray tube with λ=1.54056Å).

## 3. Results and Discussion

Figure (2) shows the XRD patterns of the three nanopowder samples prepared in this work. It is clear that the crystalline structure of the nanopowder prepared by the solvothermal method (1:1) is identical to that of nanopowder prepared by dc reactive sputtering (2:1) without heat sink step. The difference in mixing ratio between these samples is attributed to the higher transition rate from anatase into rutile in the solvothermal method due to the inevitable thermal effect included in such preparation method, while the dc reactive sputtering technique may include limited thermal effect resulted from the heating of anode (and hence substrate) during deposition time [9]. Consequently, the transition rate from anatase into rutile is lower than that in the solvothermal method. As shown in tables (1) and (2), another difference between these two patterns is observed in the FWHM values as the 2:1 sample shows larger values of FWHM when compared to that of the 1:1 sample. This can be ascribed to the fact that sputtering is an atomic-scale preparation method while the solvothermal method is a chemical reduction method. So, the size distribution of nanoparticles formed in sputtering technique is reasonably lower than that in solvothermal method. Wider FWHM means smaller nanoparticles within the crystalline structure [16].

**Table (1) XRD parameters of the 1:1 nanopowder sample**

| No. | Position [°2θ] | d-spacing [Å] | FWHM [°2θ] | Crystallite Size [nm] |
|---|---|---|---|---|
| 1 | 25.4315 | 3.499 | 0.1624 | 61.5 |
| 2 | 27.5239 | 3.238 | 0.0758 | 22.6 |
| 3 | 36.1697 | 2.481 | 0.0866 | 16.0 |
| 4 | 37.8389 | 2.375 | 0.0758 | 22.8 |
| 5 | 41.3361 | 2.182 | 0.0866 | 16.2 |
| 6 | 48.1359 | 1.888 | 0.1948 | 53.3 |
| 7 | 53.9573 | 1.697 | 0.1948 | 54.7 |
| 8 | 54.3939 | 1.685 | 0.0792 | 31.3 |
| 9 | 55.1386 | 1.664 | 0.1848 | 57.5 |
| 10 | 62.8176 | 1.478 | 0.1584 | 78.1 |
| 11 | 69.8624 | 1.345 | 0.0792 | 34.0 |
| 12 | 75.1086 | 1.263 | 0.1320 | 13.2 |

**Table (2) XRD parameters of the 4:1 nanopowder sample**

| No. | Position [°2θ] | d-spacing [Å] | FWHM [°2θ] | Crystallite Size [nm] |
|---|---|---|---|---|
| 1 | 25.4315 | 3.499 | 0.11368 | 43.05 |
| 2 | 27.5239 | 3.238 | 0.05306 | 15.83 |
| 3 | 36.1697 | 2.481 | 0.06062 | 11.20 |
| 4 | 37.8389 | 2.375 | 0.05306 | 16.02 |
| 5 | 41.3361 | 2.182 | 0.06062 | 11.38 |
| 6 | 48.1359 | 1.888 | 0.13636 | 37.31 |
| 7 | 53.9573 | 1.697 | 0.13636 | 38.29 |
| 8 | 54.3939 | 1.685 | 0.05544 | 21.96 |
| 9 | 55.1386 | 1.664 | 0.12936 | 40.25 |
| 10 | 62.8176 | 1.478 | 0.11088 | 54.67 |
| 11 | 69.8624 | 1.345 | 0.05544 | 23.83 |
| 12 | 75.1086 | 1.263 | 0.09240 | 09.24 |

On the other hand, the nanopowder prepared by dc reactive sputtering technique with heat sink step exhibits single phase (anatase only) structure as the thermal transition was completely prevented

throughout cooling the anode (and hence the substrate) [7]. As well, the FWHM values are comparable to those of the 2:1 nanopowder sample, as shown in table (3), which is attributed to the same reason as they are both prepared by sputtering technique.

**Table (3) XRD parameters of the anatase nanopowder sample**

| No. | Position [°2θ] | d-spacing [Å] | FWHM [°2θ] | Crystallite Size [nm] |
|---|---|---|---|---|
| 1 | 25.2293 | 3.527 | 0.2814 | 33.5 |
| 2 | 38.6007 | 2.330 | 0.2598 | 37.7 |
| 3 | 47.9753 | 1.894 | 0.1948 | 53.2 |
| 4 | 55.0723 | 1.666 | 0.1732 | 62.8 |
| 5 | 62.8468 | 1.477 | 0.4330 | 24.5 |
| 6 | 68.8081 | 1.363 | 0.4330 | 25.4 |
| 7 | 75.0583 | 1.264 | 0.5196 | 21.9 |

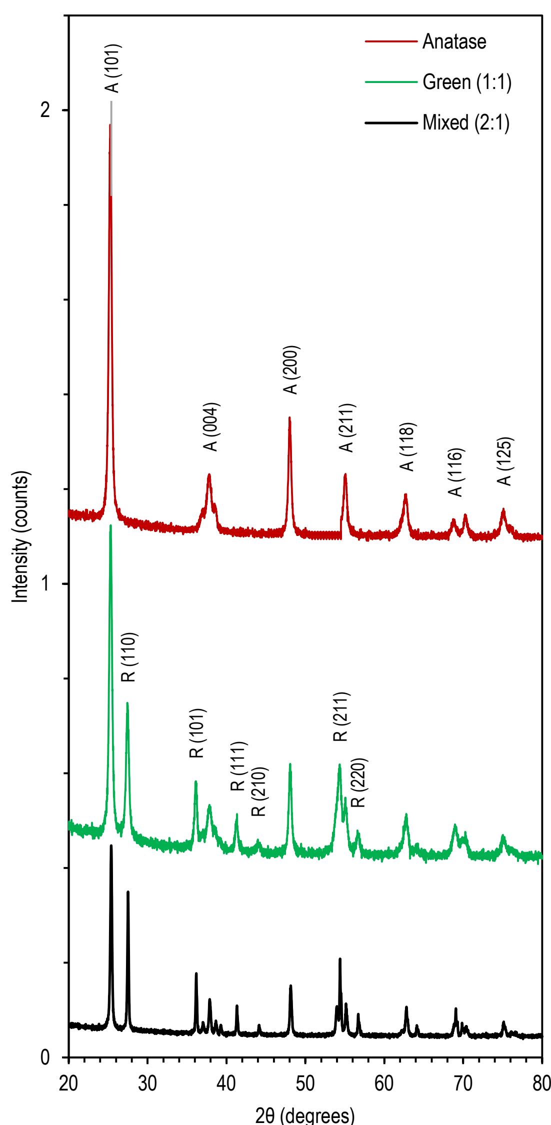


**Fig. (2) XRD patterns of the three $TiO_2$ nanopowder samples prepared in this work**

## 4. Conclusion

In concluding remarks, the crystalline structures of the $TiO_2$ nanopowders is reasonably affected by the preparation method as the preparation parameters can allow or prevent the transition of anatase phase of $TiO_2$ into rutile phase. Also, the average crystallite size is sufficiently affected by the preparation method as the dc reactive sputtering technique may produce mixed-phase $TiO_2$ nanopowder with higher anatase content and lower crystallite size. Accordingly, preparation method has an important role in determining the structural characteristics of the $TiO_2$ nanopowder and hence the preparation parameters should be sufficiently governed in order to control these characteristics.

## References

[1] S. Rehman et al., “Strategies of making $TiO_2$ and ZnO visible light active”, J. Hazard. Mater., 170(2-3) (2009) 560-569.

[2] A.L. Linsebigler, G. Lu, and J.T. Yates, “Photocatalysis on $TiO_2$ Surfaces: Principles, Mechanisms, and Selected Results”, Chem. Rev., 95(3) (1995) 735-758.

[3] N.T. Nolan, “Sol-Gel Synthesis and Characterization of Novel Metal Oxide Nano-materials for Photocatalytic Applications”, Ph.D. thesis, Dublin Institute of Technology, Ireland (2010).

[4] K. Eufinger, “Effect of deposition conditions and doping on the structure, optical properties and photocatalytic activity of d.c. magnetron sputtered $TiO_2$ thin films”, Ph.D. thesis, Ghent University, Belgium (2007).

[5] O. Carp, C.L. Huisman and A. Reller, “Photoinduced reactivity of titanium dioxide”, Prog. Sol. Stat. Chem., 32 (2004) 33-117.

[6] O.A. Hammadi, F.J. Kadhim and E.A. Al-Oubidy, “Photocatalytic Activity of Nitrogen-Doped Titanium Dioxide Nanostructures Synthesized by DC Reactive Magnetron Sputtering Technique”, Nonl. Opt. Quantum Opt., 51(1-2) (2019) 67-78.

[7] E.A. Al-Oubidy and F.J. Al-Maliki, “Photocatalytic activity of anatase titanium dioxide nanostructures prepared by reactive magnetron sputtering technique”, Opt. Quantum Electron., 51(1-2) (2019) 23.

[8] E.A. Al-Oubidy and F.J. Al-Maliki, “Effect of Gas Mixing Ratio on Energy Band Gap of Mixed-Phase Titanium Dioxide Nanostructures Prepared by Reactive Magnetron Sputtering Technique”, Iraqi J. Appl. Phys., 14(4) (2018) 19-23.

[9] F.J. Al-Maliki, O.A. Hammadi and E.A. Al-Oubidy, “Optimization of Rutile/Anatase Ratio in Titanium Dioxide Nanostructures prepared by DC Magnetron Sputtering Technique”, Iraqi J. Sci., 60(special issue) (2019) 91-98.

 © All Copyrights are reserved 

[10] F.J. Al-Maliki and E.A. Al-Oubidy, "Effect of gas mixing ratio on structural characteristics of titanium dioxide nanostructures synthesized by DC reactive magnetron sputtering", Physica B: Cond. Matter, 555 (2019) 18-20
[11] F.J. Al-Maliki, O.A. Hammadi, B.T. Chiad and E.A. Al-Oubidy, "Enhanced photocatalytic activity of Ag-doped $TiO_2$ nanoparticles synthesized by DC Reactive Magnetron Co-Sputtering Technique", Opt. Quantum Electron., 52 (2020) 188.
[12] R.A.H. Hassan and F.T. Ibrahim, "Preparation and Characterization of Anatase Titanium Dioxide Nanostructures as Smart and Self-Cleaned Surfaces", Iraqi J. Appl. Phys., 16(4) (2020) 13-18.
[13] M.A. Hameed, S.H. Faisal, R.H. Turki, "Characterization of Multilayer Highly-Pure Metal Oxide Structures Prepared by DC Reactive Magnetron Sputtering Technique", Iraqi J. Appl. Phys., 16(4) (2020) 25-30
[14] Z.H. Zaidan, K.H. Mahmood and O.A. Hammadi, "Using Banana Peels for Green Synthesis of Mixed-Phase Titanium Dioxide Nanopowders", Iraqi J. Appl. Phys., 18(4) (2022) 27-30.
[15] O.A. Hammadi, "Production of Nanopowders from Physical Vapor Deposited Films on Nonmetallic Substrates by Conjunctional Freezing-Assisted Ultrasonic Extraction Method", Proc. IMechE, Part N, J. Nanomater. Nanoeng. Nanosys., 232(4) (2018) 135-140.
[16] A. Zachariah et al., "Synergistic Effect in Photocatalysis As Observed for Mixed-Phase Nanocrystalline Titania Processed via Sol-Gel Solvent Mixing and Calcination", J. Phys. Chem. C, 112 (2008) 11345-11356.

# Analysis of X-ray Diffraction Patterns of Carbon Nitride Nanopowders Prepared by Fast Glow Discharge-Induced Reaction

**Sami M. Abdullah[1], Oday A. Hammadi[2], Laith R. Ghareeb[1]**

[1] Department of Physics, College of Science, University of Sumer, Thi Qar, IRAQ
[2] Department of Physics, College of Education, Al-Iraqia University, Baghdad, IRAQ

**Abstract**
In this work, the reaction of methane and ammonia gases at room temperature was induced by electric power transferred to the reaction volume throughout argon fast glow discharge at high pressures. This power was applied to the reaction as short pulses to produce carbon nitride nanoparticles without production of cyanogen molecules. The growth and development of carbon nitride structures was confirmed by x-ray diffraction (XRD) and Fourier-transform infrared (FTIR) spectroscopy. The synthesized carbon nitride nanoparticles were polycrystalline and lower number of crystal planes was obtained using shorter pulses of discharge power.

**Keywords:** Carbon nitride; Nanoparticles; Glow discharge; Structural characteristics
**Received**: 22 February 2023; **Revised:** 16 May 2023; **Accepted:** 24 May 2023; **Published:** 1 June 2023

## 1. Introduction

Due to the increasing importance of carbon nitride nanostructures in various applications, intense research works were carried out during the last two decades on the synthesis as well as characterization of such structures. This compound is very interesting candidate for applications such nanocomposite with enhanced photocatalytic activity [1], nanocomposites [2], electrocatalyst [3], photochemical applications such as photoredox catalysis [4], metal-free catalysis [5-7], optoelectronics such as photodiodes [8] and tribology [9].

Carbon nitride has many formulas resulted from the bonding of carbon and nitrogen atoms, however, dicyanodiazomethane with the formula of $C_3N_4$ or $(CN)_2.C.N_2$ is one of the most important ones and has a 3D structure as shown in Fig. (1) [10,11]. It has two solid covalent network compounds: beta ($\beta$-$C_3N_4$) and graphitic (g-$C_3N_4$). The first is predicted to be harder than diamond while the second has very important catalytic properties [12-15].

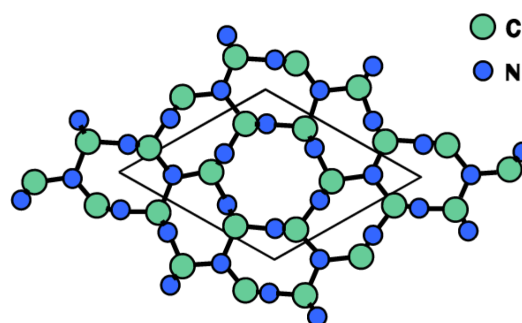


**Fig. (1) The chemical structure of dicyanodiazomethane ($C_3N_4$) molecule**

Carbon nitride nanostructures are synthesized and prepared by various methods and techniques such as photoreduction [1], thermal evaporation [3], polymerization of some organic compounds [5,13], laser ablation in liquids [6], chemical vapor deposition [10], plasma decomposition of methane and molecular nitrogen [11], ball-milling at high temperatures [15], plasma-enhanced chemical vapor deposition [9,12,17], laser pyrolysis [18], RF reactive magnetron sputtering [19], ion beam assisted sputtering [20] and shock-wave compression of organic C-N-H precursors [11].

In a total reaction volume of 2000 mm$^3$ and gas pressure 5 mbar, the reaction of methane ($CH_4$) and ammonia ($NH_3$) needs for more

 © All Copyrights are reserved 

than 5 ms to occur normally at room temperature and lead to the formation of cyanogen ($C_2N_2$) as follows [21-24]:

$$2CH_4 + 2NH_3 \rightarrow C_2N_2 + 7H_2 \quad (1)$$

The chemical structure of cyanogen includes triple bonds between carbon and nitrogen atoms in the form N≡C-C≡N. It is very hazardous and flammable compound [21,24].

The final product of this reaction can be varied by controlling the molar concentrations of starting materials as well as providing high power as short pulses to the reactants [5,8,17]. Then, dicyanodiazomethane ($C_3N_4$) can be formed as follows [25,26]:

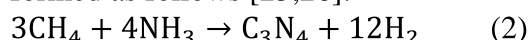

$$3CH_4 + 4NH_3 \rightarrow C_3N_4 + 12H_2 \quad (2)$$

The bonds between nitrogen (N) and hydrogen (H) atoms in ammonia molecule as well as those between carbon (C) and hydrogen (H) atoms in methane molecule can be easily broken by high power provided by the glow discharge [23]. Therefore, the released carbon and nitrogen atoms tend to bond with the availability of these atoms at high pressures (~3mbar).

In this work, carbon nitride ($C_3N_4$) nanoparticles are synthesized by a novel technique including fast glow discharge of methane and ammonia gas mixtures at high

## 2. Experimental Part

Deposition camber is first evacuated down to $10^{-5}$ mbar to remove any residuals or contaminants. Argon gas at pressure of 0.5 mbar was used to generate the fast glow discharge between two electrodes made of stainless steel. The dimensions of each electrode are 20x5 $mm^2$. Argon was chosen due to its low breakdown voltage (~190V at 35mA) compared to methane and ammonia, therefore, small amount (~0.033%) of the minimum applied power is consumed for the generation of plasma column to represent the resistor through which the remaining power (~99.96%) is transferred to the reaction volume to break the bonds in methane and ammonia molecules and soon induce the reaction between the released carbon and nitrogen atoms. The discharge power from a power supply (5-6kV, 4-5A) is applied between the electrodes as pulses of different durations (0.1, 0.25 and 1ms). A pulse forming network (PFN) was used to convert the DC signal of the power supply into short pulses. The repetition rate of discharge pulses could be determined from 1 to 100 Hz by the PFN circuit. However, all results presented here were obtained using repetition rate of 20 Hz. The methane ($CH_4$) and ammonia ($NH_3$) gases are premixed in a cooled reactor before pumped into the chamber at flow rate of 1 sccm. This reactor is cooled down to 5°C to prevent the normal reaction of methane and ammonia (Eq. 1). The maximum pressure of gas mixture is 3 mbar. As soon as the breakdown of argon gas occurs, the remaining power induces the reaction (Eq. 2) between $CH_4$ and $NH_3$ molecules to form $C_3N_4$ molecules. This reaction occurs faster than the normal reaction given by Eq. 1. The synthesized nanoparticles were collected on a clean watch glass (2cm in diameter) inside the chamber. The chamber was kept closed during the application of discharge power throughout valves on the inlets of gases and outlet to the vacuum pump. Figure (2) shows the $C_3N_4$ nanopowder sample prepared in this work.

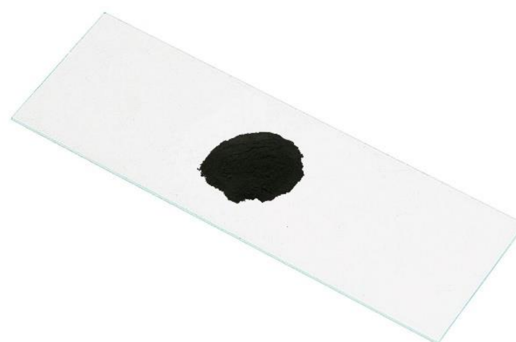

**Fig. (1) Photograph of carbon nitride nanopowder prepared by in this work**

## 3. Results and Discussion

Figure (3) shows the XRD patterns of the synthesized carbon nitride samples using fast glow discharge pulses of different durations. These patterns were illustrated with CrystalSleuth® software for XRD analysis. The sample synthesized using glow discharge pulse duration of 1 ms (Fig. 3a) shows that it is polycrystalline with twelve distinguished peaks corresponding to the crystal planes of

 © All Copyrights are reserved 

(110), (200), (101), (210), (111), (300), (220), (310), (400), (221), (311) and (320) [1,5,18,27-30]. The number of these peaks was decreased to seven while the heights of the observed peaks were increased as the discharge pulse duration is decreased to 0.25 ms (Fig. 3b). Moreover, only three peaks are observed in the synthesized sample as the discharge pulse duration is decreased to 0.1 ms (Fig. 3c). The heights of the three observed peaks were increased. This result may be attributed to the fact that some crystal planes does not find enough time to grow at shorter pulse durations, while some other planes, such as (110), (200) and (111), are immediately formed. In other words, if the discharge power of 20-30 kW is transferred to the reaction volume during shorter time, the crystal planes produced by the reaction leading to form $C_3N_4$ molecules are fewer than those produced at relatively longer time. Accordingly, the crystal planes of (110), (200) and (111) seem to grow as soon as the carbon and nitrogen atoms are bonded to form $C_3N_4$ molecules.

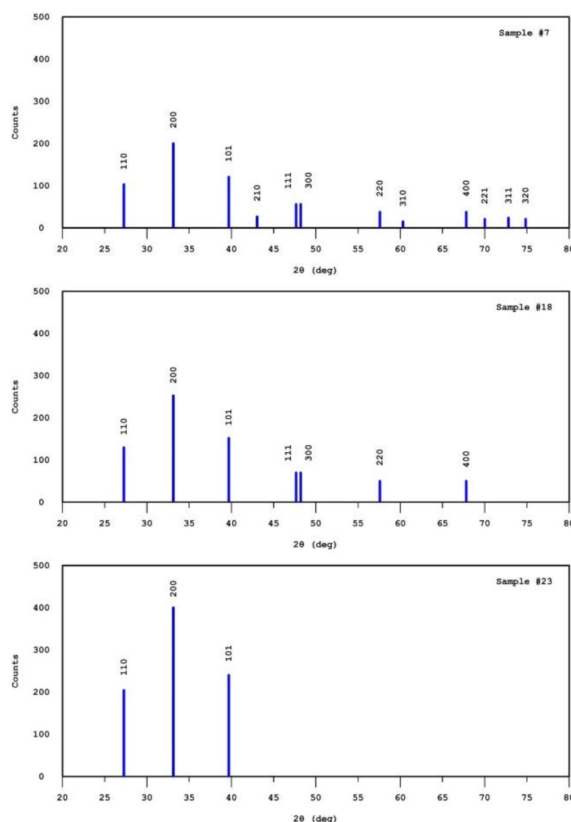

**Fig. (2) The x-ray diffraction (XRD) patterns for the synthesized samples using discharge pulse duration of (upper) 1 ms, (middle) 0.25 ms, and (lower) 0.1 ms**

Figure (4) shows the FTIR spectrum of the carbon nitride sample synthesized by discharge pulse duration of 0.1 ms. The broad band around 1100-1250 $cm^{-1}$ is attributed to the stretching mode of C-N bond [5]. However, the peak at 1250 $cm^{-1}$ is a characteristic for the $sp^3$-bonded C-N [8]. The peak around 1550 $cm^{-1}$ is ascribed to the stretching mode of double C=N bond [9]. The peak around 1600 $cm^{-1}$ is also attributed to the stretching vibration of C-N bond [13]. These peaks can be overlapped with other peaks within 1000-1800 $cm^{-1}$ ascribed to the bonded carbon layers, which become active in the infrared region as their symmetry is broken due to the incorporation of nitrogen in these layers [30]. The peaks observed below 950 $cm^{-1}$ are attributed to the C-H bond [8,31]. Other peaks observed around 2900 and 3340 $cm^{-1}$ are attributed to the $CH_x$ and $NH_x$ groups, respectively, as precursors of carbon nitride molecules.

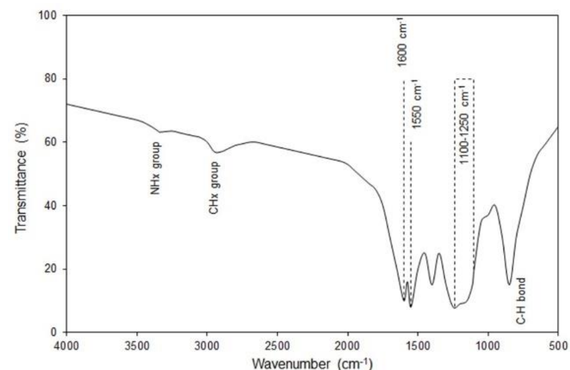

**Fig. (4) The FTIR spectrum for the carbon nitride sample synthesized using discharge pulse duration of 0.1 ms**

## 4. Conclusion

In concluding remarks, the reaction of methane ($CH_4$) and ammonia ($NH_3$) gases can be induced and controlled towards the production of carbon nitride ($C_3N_4$) nanoparticles without formation of cyanogen ($C_2N_2$). This control is performed by the application of high discharge power as short pulses to the reaction volume. The discharge pulse duration was found very important to control the number of crystal planes formed in the final product.

 © All Copyrights are reserved 

## References

[1] X. Yuan, C. Zhou, Q. Jing, Q. Tang, Y. Mu and A. Du, *Nanomater.*, 6 (2016) 173.
[2] E.M. Fayyad, A.M. Abdullah, M.K. Hassan, A.M. Mohamed, C. Wang, G. Jarjoura and Z. Farhat, *Coatings*, 8 (2018) 37.
[3] F. Liu, Y. Ren and X. Ji, *Int. J. Mater. Sci. Eng.*, 5(4) (2017), 123-132.
[4] Dandan Zheng, Xu-Ning Cao, and Xinchen Wang, *Angew. Chem. Int. Ed.*, 55 (2016) 11512 –11516.
[5] A. Thomas, A. Fischer, F. Goettmann, M. Antonietti, J.-O. Müller, R. Schlögl and J.M. Carlsson, *J. Mater. Chem.*, 18 (2008) 4893-4908.
[6] Y. Zhao, F. Zhao, X. Wang, C. Xu, Z. Zhang, G. Shi and L. Qu, *Angew. Chem. Int. Ed.*, 53 (2014) 13934–13939.
[7] S. Elavarasan, B. Baskar, C. Senthil, Piyali Bhanja, A. Bhaumik, P. Selvam and M. Sasidharan, *RSC Adv.*, 6 (2016) 49376-49386.
[8] K.S. Khashan and M.H. Mohsin, *Surf. Rev. Lett.*, 22(4) (2015) 1550055.
[9] J. Ni and X. Hao, *Adv. Mater. Res.*, 538-541 (2012) 124-127.
[10] P.W. May, P.R. Burridge, C.A. Rego, R.S. Tsang, M.N.R. Ashfold, K.N. Rosser, R.E. Tanner, D. Cherns and R. Vincent, *Diam. Rel. Mater.*, 5 (1996) 354-358.
[11] C.M. Lieber and J. Zhang, *Adv. Mater.*, 6(6) (1994) 497-499.
[12] W.T. Zheng, X. Wang, T. Ding, X.T. Li and W.D. Fei, *Int. J. Mod. Phys. B*, 6(6-7) (2002) 1091-1095.
[13] E. Kovačević, J. Berndt, I. Stefanović, H.-W. Becker, C. Godde, Th. Strunskus, J. Winter and L. Boufendi, *J. Appl. Phys.*, 105 (2009) 104910.
[14] J.V. Badding and D.C. Nesting, *Chem. Mater.*, 8(2) (1996) 535-540.
[15] Z.Y. Fei and Y.X. Liu, *Chin. Phys. Lett.*, 20(9) (2003) 1554-1557.
[16] O.A. Hamadi, *Iraqi J. Appl. Phys. Lett. (IJAPLett)*, 1(2) (2008) 3-8.
[17] J. G. Céspedes, C. Corbella, E. Bertran, G. Viera & M. Galán, *Fullerenes, Nanotubes and Carbon Nanostructures*, 13(1) (2007) 447-455.
[18] R. Alexandrescu, F. Huisken, G. Pugna, A. Crunteanu, S. Petcu, S. Cojocaru, R. Cireasa and I. Morjan, *Appl. Phys. A*, 65 (1997) 207-213.
[19] W.T. Zheng, J.J. Li, X. Wang, X.T. Li, Z.S. Jin, B.K. Tay and C.Q. Sun, *J. Appl. Phys.*, 49(4) (2003) 2741-2745.
[20] P. Hammer, M.A. Baker, C. Lenardi and W. Gissler, *Thin Solid Films*, 290-291 (1996) 107-111.
[21] R.A. Meyers (Editor), **“Encyclopedia of Physical Science and Technology: Inorganic Chemistry”**, 3rd ed., Academic Press (2003), 828-829.
[22] P.A. Gartaganis and C.A. Winkler, *Canad. J. Chem.*, 34 (1956) 1457-1463.
[23] S.L. Miller, *Biochimica et Biophysica Acta*, 23 (1957) 480-489.
[24] P. Carson and C. Mumford, **“Hazardous Chemicals Handbook”**, Butterworth-Heinemann (Oxford, 2002), 2nd ed., 156, 233.
[25] C. Niu, Y.Z. Lu and C.M. Lieber, *Science*, 261(5119) (1993) 334-337.
[26] L.-W. Yin, M.-S. Li, Y.-X. Liu, J.-L. Sui and J.-M. Wang, *J. Phys.: Cond. Matter*, 15(2) (2003) 309-314.
[27] O. Matsumoto, T. Kotaki, H. Shikano, K. Takemura and S. Tanaka, *J. Electrochem. Soc.*, 141(2) (1994) L16-L18.
[28] Y. Gu, Y. Zhang, X. Chang, Z. Tian, N. Chen, D. Shi, X. Zhang and L. Yuan, *Sci. China Ser. A-Math.*, 43(2) (2000) 185-198.
[29] M. Arif, L.N. Blinov, R. Lappalainen and S.N. Filippov, *Glass Phys. Chem.*, 30(6) (2004) 573-575.
[30] H. Wang, “Investigations into Carbon Nitrides and Carbon Nitride Derivatives”, PhD thesis, University of Munchen (Germany, 2013).
[31] V.P. Tolstoy, I.V. Chernyshova and V.A. Skryshevsky, **“Handbook of Infrared Spectroscopy of Ultrathin Films”**, Wiley-Interscience (NJ, 2003), 439
[32] O.A. Hamadi, *Proc. IMechE, Part L, Journal of Materials: Design and Applications*, 222 (2008) 65-71.
[33] A.K. Yousif and O.A. Hamadi, Bulgarian J. Phys., 35(3) (2008) 191-197.
[34] O.A. Hammadi, W.N. Raja, M.A. Saleh and W.A. Altun, *Iraqi J. Appl. Phys. (IJAP)*, 12(3) (2016) 35-42.
[35] O.A. Hammadi, *Photonic Sensors*, 6(4) (2016) 345-350.

# Effect of Magnetron Configuration on Plasma Parameters in Sputtering Technique

**Mohammed A. Hussain[1], Ali M. Ghafoori[1], Omar S. Habeeb[2]**

[1] Department of Electrical Engineering, College of Engineering, University of Anbar, Ramadi, IRAQ
[2] Department of Software Engineering, College of Engineering, University of Baghdad, Baghdad, IRAQ

**Abstract**
In this work, a closed-field unbalanced dual magnetron assembly was designed, constructed and characterized. This assembly can be successfully used in plasma sputtering system to improve the electrical characteristics of the plasma. This improvement was shown by the Langmuir probe diagnostics of the plasma and the values of plasma parameters, such as electron and ion temperatures and densities. The applicability of such design may enhance the whole sputtering process and the production of nanoscale structures with low cost, high purity and good properties.

**Keywords:** Magnetron sputtering; Plasma parameters; Langmuir diagnostics; Glow discharge
**Received**: 02 February 2023; **Revised:** 08 May 2023; **Accepted:** 15 May 2023; **Published:** 1 June 2023

## 1. Introduction

Sputtering is complex process, which is highly dependent on number of process parameters, such as deposition pressure, discharge voltage, discharge current, target to substrate distance, gas compositions, process gas flow rate, reactive gas flow rate in case of reactive sputtering, substrate biasing, etc. [1-7]. Deposition of thin films by magnetron-based sputtering systems is performed at much higher rates than diodes and operated at lower pressures, where gas-phase scattering and gas-phase impurities are minimal [8-10]. DC magnetron is basically a magnetically enhanced diode in which the spatial relationship of electric and magnetic field is designed to confirm secondary electrons produced by ions bombardment of the target [11-13]. Restricting these electrons to remain close to the target surface increases their probability to ionize the working gas [14]. This effect results in more intense plasma discharge that can be sustained at lower pressure. Since the ions are heavier than electrons, they are not affected by the confining magnetic field and may sputter much as in a diode type configuration [15,16].

In case of planar circular magnetron – which is used in the present work – two round magnets are placed behind the target, as can be seen in the figure below and formation of an erosion profile known as “racetrack” is induced by the non-uniform ion bombardment across the target surface [17,18]. For balanced magnetrons, both magnets have the same magnet strength that results in strongly confined plasma near the target region [19]. Consequently, only a few charged particles reach the substrate, which might be useful in the case where low energetic bombardment is mandatory as in the case of polymeric substrates, but it is a drawback when energetic ion/electron bombardment in the anode surface is needed because the bombardment with energetic particles (ions or electrons) influence the growth of thin films [20-22].

The bombardment of the substrate with energetic particles can be achieved by unbalanced magnetron configuration, as two magnets with different strength and/or dimensions are used [23,24]. This way, the magnetic field lines are extended to the substrate and the plasma density is increased near the substrate [25-27]. Although the presence of magnets increases the efficiency of sputtering, it leads to inefficient target usage where only ~30% of the material is used [28-30].

The bulk of the plasma is “quasineutral” where electron and ion densities are the same,

 © All Copyrights are reserved 

and the potential difference between the bulk of the plasma and the wall is concentrated in a thin layer or sheath near the wall [31]. The gradient of the plasma potential determines the electric field that is responsible for energizing the electrons, which maintain the discharge through ionization [32].

In this work, a closed-field unbalanced dual magnetron assembly was designed, constructed and characterized to be used in plasma sputtering system to improve the electrical characteristics of the plasma. This improvement was shown by the Langmuir probe diagnostics of the plasma and the values of plasma parameters, such as electron and ion temperatures and densities.

## 2. Experimental Part

Two closed-field unbalanced magnetrons were employed at the anode and cathode of plasma sputtering system. Electrodes (anode and cathode) were made of stainless steel and each was a disk of 8 cm in diameter and 4 mm in thickness. Two annular concentric magnets were placed behind each electrode to form the magnetron configuration. The outer diameters of the two magnets were 8 cm and 4 cm, while the inner diameters were 4 cm and 3.2, respectively. The electrodes were connected to a DC power supply to provide the electrical power required for discharge. The lower electrode (anode) could be move vertically with respect to the fixed upper electrode (cathode) to adjust the separation of the two electrodes from 1 to 8 cm.

Pure argon gas was used to produce the discharge plasma. A DC power supply up to 5 kV was used for electrical discharge between the electrodes and both breakdown voltage (up to 1 kV) and discharge current (up to 100 mA) were monitored by two digital voltmeter and ammeter, respectively. A current limiting resistor of 6.75 kW was connected in series to the discharge circuit in order to control the current flowing in the circuit. The discharge chamber was evacuated by a two-stage Leybold-Heraeus rotary pump and the vacuum inside chamber was measured by Pirani gauge connected to a vacuum controller from Balzers VWS 120. Argon gas was supplied to the chamber through a fine-controlled needle valve (0-160 ccm) to control the gas pressure inside the chamber.

## 3. Results and Discussion

When dual magnetrons were used, the drained current by the probe was decreased by about 16% due to the roles of both magnetrons in trapping much more charged particles near the cathode and anode and hence reducing the number of particles passing the distance between the electrodes where the probe is placed. However, these roles could not prevent the discharge current from flowing between the electrodes but even these particles sustaining the discharge are accelerated by the both electric and magnetic fields to higher drift velocities that the probe could not attract them from their paths across the inter-electrode distance [33].

Accordingly, the magnetrons caused to change the values of plasma parameters, such as electron and ion temperatures and densities, as these parameters are deduced from the current-voltage characteristics of the probe immersed in plasma. These variations are observed in Table (1).

**Table (1) Effect of using magnetrons on the plasma parameters**

| | No magnetron | One magnetron | Dual magnetrons |
|---|---|---|---|
| Electron Temperature (eV) | 4.856 | 4.871 | 4.850 |
| Electron Density ($x10^{21}m^{-3}$) | 1.329 | 1.148 | 1.130 |
| Ion Temperature (eV) | 0.889-1.192 | 0.888-1.189 | 0.864-1.159 |
| Ion Density ($x10^{21}m^{-3}$) | 1.329 | 1.148 | 1.130 |

The probe current near the anode was higher by about 6% than its value at the center point because the density of electrons near the anode is already low and the magnetron at the anode also plays a role in trapping a fraction of these electrons near the anode. Therefore, the number of electrons collected by the probe near the anode is reasonably lower than that that near the cathode [34].

For comparison, the electron temperatures and densities were determined from the current-voltage characteristics of Langmuir probe for three different working pressures and at the center point between the electrodes. As shown in Fig. (1), the electron temperature was reduced as the working pressure increased from 0.35 to 0.7mbar and then raised as the pressure increased from 0.7 to 0.9mbar.

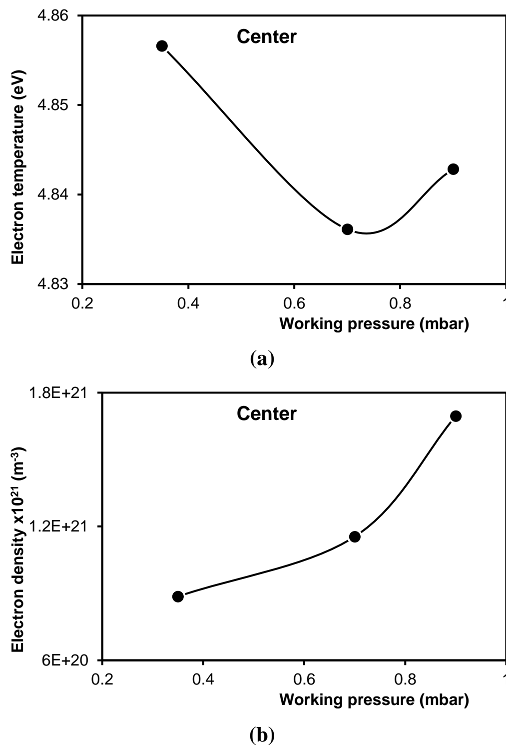


**Fig. (1) Variation of electron temperature and density in plasma with working gas pressure at the center point between the electrodes when dual magnetrons were used**

Increasing the working pressure means providing the discharge volume with more neutral atoms of argon and hence the mean free path of electrons as well as their gained energy is reduced as the number of their collisions with neutral atoms is decreased. Accordingly, the number of electrons produced by collisional ionization processes is decreased. The majority of these electrons are trapped by the magnetrons at both electrodes while the minority of electrons may escape from the trapping region towards the anode to sustain the glow discharge with lower energies (lower temperatures) than those trapped because they will be subject only to the electric field between the electrodes (V/d) while those trapped near the electrodes are subject to ExB drift.

A fraction of the electrons escaping from ExB trapping region may be collected by the probe at the center point between the electrodes to form the probe current, which was shown lower than those near the electrodes.

The further increase of working pressure (to 0.9mbar) provide the discharge volume with more neutral gas atoms, therefore, the number of collisions among electrons and neutral atoms is increased and hence the production of charged particles is increased too. Accordingly, the electron density is increased and more electrons are trapped by ExB effect before escaping to pass the inter-electrode distance as well as the center point where the probe is placed. These electrons are relatively higher in energy than those escaping at lower pressures (0.7mbar) because they were initially trapped before the electron density being higher than the capability of trapping region. Therefore, the probe would collect more electrons with higher energies (temperatures). Despite that ion temperatures are much lower than electron temperatures; similar behavior was observed when measured at different points between the electrodes [35].

On the other hand, the electron density (as well as ion density) was continuously increased with increasing working pressure due to the corresponding increase in discharge current, as shown earlier. The following table shows the plasma parameters deduced at three different positions between the discharge electrodes.

**Table (2) Plasma parameters measured at three different positions between the discharge electrodes**

| | Center point | Near cathode | Near anode |
|---|---|---|---|
| Electron Temperature (eV) | 4.856 | 4.838 | 4.855 |
| Electron Density ($x10^{21}m^{-3}$) | 1.130 | 1.654 | 1.201 |
| Ion Temperature (eV) | 0.864-1.159 | 0.885-1.188 | 0.869-1.166 |
| Ion Density | 1.130 | 1.654 | 1.201 |

 © All Copyrights are reserved 

| ($x10^{21} m^{-3}$) | | | |
|---|---|---|---|

## 4. Conclusion

The probe current was higher than other positions because the densities of electrons near the cathode are higher than any other region inside plasma since the cathode is the source of discharge electrons in addition to the trapping effect of the magnetron placed at the cathode. Therefore, the probe would collect much more electrons in this region. The increase in probe current near the cathode was about 46% than its value at the center point between the electrodes.

The probe current near the anode was higher by about 6% than its value at the center point because the density of electrons near the anode is already low and the magnetron at the anode also plays a role in trapping a fraction of these electrons near the anode. Therefore, the number of electrons collected by the probe near the anode is reasonably lower than that that near the cathode.

## References

[1] M. Lieberman, A. Lichtenberg, **Principle of plasma discharge and Material**, New York, John-Wiley and Sons (1994).
[2] G. Seriamni et al., “plasma Charactersation of a DC closed field magnetron sputtering device”, ECA, 24B, 17 (2000).
[3] M. Ghoranneviss et al., “The effect of parameter of plasma of DC magnetron sputtering on properties of copper thin film deposited on glass”, XXVIIth ICPIG, Eindhoven, Netherlands (2005).
[4] C. Shon et al., IEEE Transactions on plasma science", 26(6) (1998).
[5] B. Chapman, **Glow Discharge Processes**, John-Wiley & Sons, NY (1980).
[6] R. Berry, P. Hall, and M. Harris, **Thin Film Technology**, van Nostrand Reinhold Company, New York (1968).
[7] K. Hinkel, **Magnetrons**, Cleaver-Hume Press Ltd., London, 1961.
[8] J. Vossen, **Thin Film Processes**, Academic Press, Inc., New York (1978).
[9] K. Wasa and S. Hayakawa, Rev. Sci. Instrum., 40(5) (1969) 693.
[10] B. Subramanian et al., Surf. Coat. Technol., 205(21-22) (2011) 5014–5020.
[11] A. Grill, **Cold Plasma in Materials Fabrication**, IEEE, New York, 1994.
[12] N. Kumari et al., Euro. Phys. J., 59(2) (2012), Article ID 20302, 7 pages.
[13] J.A. Thornton, J. Vac. Sci. Technol., 15(2) (1978) 171–177.
[14] S.Z. Wu, J. Appl. Phys., 98 (2005), Article ID 083301, 5 pages.
[15] T.E. Sheridan, M.J. Goeckner and J. Goree, J. Vac. Sci. Technol. A, 8(30) (1990) 8 pages.
[16] S.L. Rohde et al., Thin Solid Films, 193-194(1) (1990) 117–126.
[17] R.P. Howson, H.A. J’Afer and A.G. Spencer, Thin Solid Films, 193-194(1) (1990) 127–137.
[18] S.M. Borah et al., J. Phys. D: Appl. Phys., 41(19) (2008), Article ID 195205.
[19] X.B. Zhang, J.Q. Xiao, Z.L. Pei, et al., J. Vac. Sci. Technol. A 25, 209 (2007).
[20] I. Petrov, F. Abibi, J.E. Greene, et al., J. Vac. Sci. Technol. A 10, 3283 (1992).
[21] I. Ivanov, P. Kazansky, L. Hultman, et al., J. Vac. Sci. Technol. A 12, 314 (1994).
[22] S.M. Rossnagel and H.R. Kaufman, J. Vac. Sci. Technol. A 4, 1822 (1986).
[23] T.E. Sheridan and J. Goree, J. Vac. Sci. Technol. A 7, 1014 (1989).
[24] I. Petrov, I. Ivanov, V. Orlinov, and J. Kourtev, Contrib. Plasma Phys. 30, 223 (1990).
[25] P. Spatenka, J. Vlcek, and J. Blazek, Vacuum 55, 165 (1999).
[26] L. Gu and M.A. Lieberman, J. Vac. Sci. Technol. A 6, 2960 (1988).
[27] S. Miyake, N. Shimura, T. Makabe and A. Itoh, J. Vac. Sci. Technol., A10, 1135 (1992).
[28] Q.A. Abbas, R.R. Abdula, B.T. Chiad, Iraqi J. Phys., 8(11) (2010) 41-47.
[29] B.T. Chied, R.R. Abdula, Q.A. Abbas, Iraqi J. Phys., 8(11) (2010) 33-40.
[30] S.M. Borah, J. Materials, 2013, Article ID 852859.
[31] A.A. Solov’ev et al., Plasma Physics Reports, 35(5) (2009) 399–408.
[32] E.F. Kotp and A.A. Al-Ojeery, Australian J. Basic Appl. Sci., 6(3) (2012) 817-825.
[33] B.T. Chiad, M.K. Khalaf, F.J. Kadhim, O.A. Hammadi, Characteristics and Operation Conditions of a Closed-Field Unbalanced DC Magnetron Plasma Sputtering System, J. Ind. Eng. Sci., accepted for publication, to appear in 2015
[34] M.K. Khalaf, O.A. Hammadi, F.J. Kadhim, Representation of Magnetic Field Distribution of Dual Closed-Field Unbalanced Magnetrons Employed in Glow-Discharge Plasma Sputtering System, submitted to Photonic Spectra, 2014.
[35] F.J. Kadhim, M.K. Khalaf, O.A. Hammadi, Optical and Structural Properties of Nickel Oxide Thin Films Prepared by Closed-Field Unbalanced Dual-Magnetrons Sputtering Technique, J. Optoelectron. Photon., accepted for publication, to appear in 2015.

**COPYRIGHT RELEASE FORM**

IRAQI JOURNAL OF
APPLIED PHYSICS LETTERS ( IJAPLett )

We, the undersigned, the author/authors of the article titled
……………………………………………………………………………………………………………………
……………………………………………………………………………………………………………………
……………………………………………………………………………………………………………………
……………………………………………………………………………………………………………………
……………………………………………………………………………………………………………………
……………………………………………………………………………………………………………………
……………………………………………………………………………………………………………………

that is submitted to the Iraqi Journal of Applied Physics Letters (IJAPLett) for publication, declare that we have neither taken part or full text from any published work by others, nor presented or published it elsewhere in any other journal. We also declare transferring copyrights and conduct of this article to the Iraqi Journal of Applied Physics Letters (IJAPLett) after accepting it for publication.

The authors will keep the following rights:

1. Possession of the article such as patent rights.
2. Free of charge use of the article or part of it in any future work by the authors such as books and lecture notes after informing IJAP editorial board.
3. Republishing the article for any personal purposes of the authors after taking journal permission.

To be signed by all authors:

Signature:…………………………………………………………..date: …………………………………………
Printed name: ……………………………………………………………………………………………………………

Signature:…………………………………………………………..date: …………………………………………
Printed name: ……………………………………………………………………………………………………………

Signature:…………………………………………………………..date: …………………………………………
Printed name: ……………………………………………………………………………………………………………

Correspondence author:…………………………………………………………………………………………...
……………………………………………………………………………………………………………………
Address:…………………………………………………………………………………………………………
……………………………………………………………………………………………………………………
Telephone:………………………………………………..email: …………………………………………………………

***Note: Complete and sign this form and mail it to the below address with your finally revised manuscript***

**The Iraqi Journal of Applied Physics Letters**
**P. O. Box 88052, Baghdad 12631, IRAQ**
www.iraqiphysicsjournal.com
Email: editor@iraqiphysicsjournal.com
Email: editor_ijap@yahoo.co.uk
Email: ijaplett.editor@gmail.com

**IRAQI JOURNAL OF APPLIED PHYSICS LETTERS**
**Volume (6) Issue (2) April-June 2023**

# CONTENTS

About Iraqi Journal of Applied Physics Letters (IJAPLett) 1

Instructions to Authors 2

Analysis of Paschen's Curve of Plasma Sputtering System Employing Closed-Field Unbalanced Dual Magnetron Assembly 3-6
Hasan M. Jasim, Raad H. Abd

Closed-Field Unbalanced Dual Magnetron Assembly for Plasma Sputtering Systems 7-10
Ali M. Ghafoori, Omar S. Habeeb, Mohammed A. Hussain

Effect of Preparation Method on Crystalline Structure of Titanium Dioxide Nanoparticles 11-14
Zahraa H. Zaidan, Oday A. Hammadi, Kasim H. Mahmood

Analysis of X-ray Diffraction Patterns of Carbon Nitride Nanopowders Prepared by Fast Glow Discharge-Induced Reaction 15-18
Sami M. Abdullah, Oday A. Hammadi, Laith R. Ghareeb

Effect of Magnetron Configuration on Plasma Parameters in Sputtering Technique 19-22
Mohammed A. Hussain, Ali M. Ghafoori, Omar S. Habeeb

Iraqi Journal of Applied Physics Letters (IJAPLett) Copyright Form 23

Contents 24